Frontiers in Heat and Mass Transfer (FHMT), 9, 33 (2017)
DOI: 10.5098/hmt.9.33

Global Digital Central
ISSN: 2151-8629

Frontiers in Heat and Mass Transfer

Available at www.ThermalFluidsCentral.org

MATHEMATICAL MODELLING OF UNSTEADY MHD DOUBLE-DIFFUSIVE NATURAL CONVECTION FLOW IN A SQUARE CAVITY

K. Venkatadri[a,*] S. Gouse Mohiddin[a], M. Suryanarayana Reddy[b]

[a] *Department of Mathematics, Madanapalle Institute of Technology & Science, Madanapalle, A.P, 517325, India.*
[b] *Department of Mathematic, JNTUA College of Engineering, Pulivendula, A.P, 516390, India.*

ABSTRACT

Two-dimensional unsteady laminar double-diffusive free convective flow of a conducting fluid in a thermally insulated square enclosure except the left wall has been numerically studied in presence of heat generation/absorption. The Marker and Cell (MAC) method is employed for solving non-linear momentum, energy and concentration equations and the numerical MATLAB code is validated with the previous study. The computed results are depicted graphically and discussed for various values of Rayleigh number (Ra), Hartmann number (Ha), Buoyancy ratio parameter (N), Lewis number (Le) and heat absorption/generation parameter (γ). It is observed that the rate of heat and mass transfer decreases with increasing Rayleigh number.

Keywords: *Double-diffusive, absorption/generation, Square Enclosure, MAC Method.*

1. INTRODUCTION

Natural convective fluid flows, heat and mass transfer has been receiving the considerable attention based on diverse fields in engineering and industrial applications including the wire electro-discharge machining (Murphy KD et al., 2000; Lambert TA et al., 2002), aerodynamic heating of air flow (Pei YC et al., 2014), magnetic systems (Ghasemia et al., 2011), liquid metal systems (Kakarantzas et al., 2014), thermal energy storage systems, chemical processes and drying technology etc. Based on the enormous expansion of the applicability of convection, the researchers are continuously exploring the convective heat and mass transfer effects on double-diffusive convection (Mchirgui et al., 2012), Magnetohydrodynamic convection (Elshehabey et al., 2015) under different thermosolutal boundaries. The major branches of continuum mechanics includes the Magnetohydrodynamics (MHD). Numerical studies on MHD convective flows in square enclosure has been studied by Davis (1983) and Ostrach (1988).

Recently many researchers interest on double diffusive convection flows in the enclosures. Mohan and Satheesh (2016) are numerical examination conducted of Double-Diffusive Mixed Convection Flow in a Lid-Driven Porous Cavity with Magnetohydrodynamic Effect is observed for different Aspect ratios. Kefayati et al. (2014) made a numerical work on the effect of inclined magnetic field on mixed convection of shear-thinning fluids in a square lid driven cavity under the combined effects of thermal and mass diffusion with top and bottom walls driven in same direction. Thereafter, Tapas Ray Mahapatra et al. (2013) studied double-diffusive natural convection in a lid-driven square cavity with uniform and non-uniform thermal and concentration boundary conditions in presence of buoyancy ratio. Makayssi et al. (2008) conduct analytical and numerical analysis of natural double-diffusive convection in a shallow cavity packed with power-law fluid. The effect of large density variable on thermosolutal natural convection in a square cavity was numerically examined by Sun et al. (2010). Study of the second law of thermodynamics in double diffusive convection for tilted porous cavity saturated with a binary perfect gas mixture is performed numerically. Heat and mass transfer and fluid flow patterns are discussed and graphically exhibited and analyzed the Control Volume Finite-Element Method (CVFEM) numerically by Ali Mchirgui et al. (2014). Kishan Naikoti et al. (2015) has reported a weighted residual Galerkin finite element numerical study of thermosolutal convection. Studies on double diffusive convection under the influence of Soret and Dufour effects. Multicellular flow patterns were also studied in an experimental study by Han and Kuehn (1991) and numerically simulated successfully H. Han (1991). Hillal M et al. (2015) and M. Sheikholeslami et al. (2014) have studied the natural convection heat transfer in an enclosures with magnetic field. Teamah et al. (2012) carried out the numerical investigation of double-diffusive convective flow in a shortest insulated walls on inclined rectangular cavity under the uniform magnetic field. The numerical results are presented under the influence of Rayleigh number on streamlines, isotherms and concentration contours, discussed the presented results are various parametric conditions. The numerical computations are carried out for fixed Prandtl number, Pr=0.7, Hartmann number range is 0 to 70, aspect ratio, A=2, and Lewis number, Le=2. M. Sathiyamoorthy et al. (2012). A numerical study is performed for Natural convective flow in a linearly heated adjacent walls of square enclosure in presence of inclined magnetic field, the governing equations of the problem are solved by using finite element approach. In this study, we investigate that the significant effects on the local and average Nusselt numbers on all walls influenced by magnetic field. Sivasankaran et al. (2011) conducted a numerical investigation on convective flow with Hydro-magnetic effect in a lid-driven square cavity with wavy heated vertical walls. The computed results are depicted for various combinations of phase deviation, amplitude ratio, Richardson number (Ri), and Hartmann number (Ha). The Nusselt number increases with the phase deviation up to right angle and then it

* Corresponding author. Email: venkatadri.venki@gmail.com

Global Digital Central
ISSN: 2151-8629

decreases for further enhancing in the phase deviation. If amplitude ratio is increased the heat transfer rate also increases are found in this study. Litan Kumar Saha et al. (2015) observed the effect of magnetic field in a square enclosure with wavy bottom wall and adiabatic side walls. The numerical computation is carried out by using finite element formulation (Galerkin weighted residual method). In this observation, the lid-driven cavity with wavy bottom wall can be considered as an effective heat transfer mechanism under magnetic field at larger amplitudes of wavy surface and low Richardson numbers.

The present examination of the effect of Hartmann number (Ha), Rayleigh number (Ra), Buoyancy ratio parameter (N) and Heat generation or absorption parameter depicted contours of temperature, streamlines and concentration. The mass and thermal exchanges generated in the case of co-operating thermal and concentration buoyancy effects with uniform thermal boundary conditions have been analyzed.

2. MATHEMATICAL MODELLING AND SIMULATION

The computational two dimensional physical system involving various thermal ambience of square enclosure filled with water are depicted in Fig. 1 (a). Unsteady laminar MHD double-diffusive natural convection inside a two–dimensional square cavity with uniformly heated/or insulated concentrated walls in presence of heat generation or absorption under the boundary conditions that the left wall is maintained at uniform heat flux and remaining walls are thermally insulated as shown in Fig. 1(a). The thermophysical properties of the fluid in the flow field are assumed to be constant except density. The variations of density with temperature can be calculated using Boussinesq approximation.

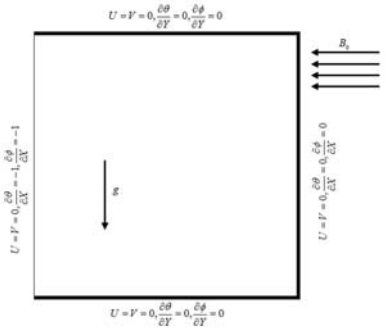

Fig. 1 (a) Schematic diagram of physical system

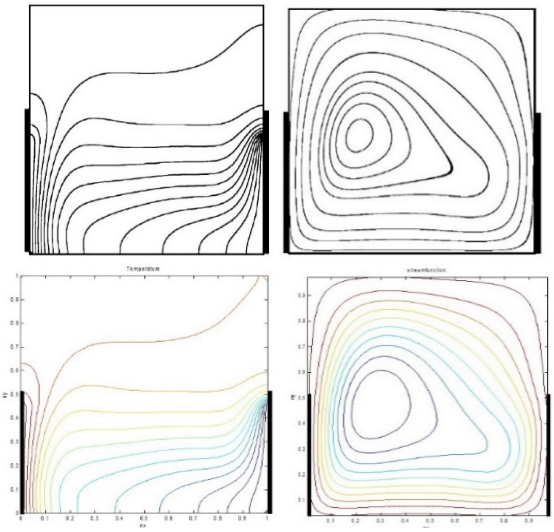

Fig. 1 (b) Comparison contour plots for bottom-bottom vertical walls with Pr=0.7, Gr = 10^5, Ha=10, Kandaswamy et al. (2008) (upper row), Present MAC computations (lower row).

The dimensional governing equations for this physical domain are based on the balance laws of mass, linear momentum, thermal energy, and concentration forms are

$$\frac{\partial u}{\partial x}+\frac{\partial v}{\partial y}=0 \tag{1}$$

$$\frac{\partial u}{\partial t}+u\frac{\partial u}{\partial x}+v\frac{\partial u}{\partial y}=-\frac{1}{\rho}\frac{\partial p}{\partial x}+\upsilon\left(\frac{\partial^2 u}{\partial x^2}+\frac{\partial^2 u}{\partial y^2}\right) \tag{2}$$

$$\frac{\partial v}{\partial t}+u\frac{\partial v}{\partial x}+v\frac{\partial v}{\partial y}=-\frac{1}{\rho}\frac{\partial p}{\partial y}+\upsilon\left(\frac{\partial^2 v}{\partial x^2}+\frac{\partial^2 v}{\partial y^2}\right)+g\beta_T\left(T-T_c\right)+g\beta_C\left(C-C_c\right)-\frac{\sigma B_0^2}{\rho}v \tag{3}$$

$$\frac{\partial T}{\partial t}+u\frac{\partial T}{\partial x}+v\frac{\partial T}{\partial y}=\alpha\left(\frac{\partial^2 T}{\partial x^2}+\frac{\partial^2 T}{\partial y^2}\right)+\frac{\varphi_0}{\rho c_p}\left(T-T_c\right) \tag{4}$$

$$\frac{\partial C}{\partial t}+u\frac{\partial C}{\partial x}+v\frac{\partial C}{\partial y}=D\left(\frac{\partial^2 C}{\partial x^2}+\frac{\partial^2 C}{\partial y^2}\right) \tag{5}$$

Where y, x and t represent vertical, horizontal distances and time respectively. u, v, T and C are the x and y directional components of velocity, pressure, temperature and concentration respectively. β_T and β_C are the thermal and solutal expansion coefficients. υ,α,ρ and c_p are the Kinematic viscosity, thermal diffusivity, fluid density and specific heat at constant pressure respectively. D is the species diffusivity, T_h and T_c are the hot and cold temperatures of wall. C_h and C_c are the concentrations at the hot and cold walls and g is gravitational acceleration. σ, B_0 and φ_0 are the electrical conductivity, magnetic induction and heat generation or absorption coefficient respectively.

The appropriate initial and boundary conditions for the problem are

$$\begin{aligned}
&x=0,\ u=v=0, -k\frac{\partial T}{\partial x}=q', -D\frac{\partial C}{\partial x}=q^*\\
&x=1,\ u=v=0, \quad \frac{\partial T}{\partial x}=0, \quad \frac{\partial C}{\partial x}=0\\
&y=0,\ u=v=0, \quad \frac{\partial T}{\partial y}=0, \quad \frac{\partial C}{\partial y}=0\\
&y=1,\ u=v=0, \quad \frac{\partial T}{\partial y}=0, \quad \frac{\partial C}{\partial y}=0
\end{aligned} \tag{6}$$

In processing the governing equations, the following non-dimensional variables are introduced:

$$\begin{aligned}
&X=\frac{x}{L}, Y=\frac{y}{L}, U=\frac{uL}{\alpha}, V=\frac{vL}{\alpha}\\
&t'=\frac{\alpha t}{L^2}, \theta=\frac{T-T_c}{\Delta T}, \phi=\frac{C-C_c}{\Delta C}, P=\frac{pL^2}{\rho\alpha^2}
\end{aligned} \tag{7}$$

where $\Delta T=\frac{q'L}{k}$ and $\Delta C=\frac{q^*L}{D}$ Equations (1)-(5) can be reduced to the following dimensionless forms by using Eq. (7)

$$\frac{\partial U}{\partial X}+\frac{\partial V}{\partial Y}=0 \tag{8}$$

$$\frac{\partial U}{\partial t'}+U\frac{\partial U}{\partial X}+V\frac{\partial U}{\partial Y}=-\frac{\partial P}{\partial X}+\Pr\left(\frac{\partial^2 U}{\partial X^2}+\frac{\partial^2 U}{\partial Y^2}\right) \tag{9}$$

$$\frac{\partial V}{\partial t'}+U\frac{\partial V}{\partial X}+V\frac{\partial V}{\partial Y}=\Pr\left(\frac{\partial^2 V}{\partial X^2}+\frac{\partial^2 V}{\partial Y^2}\right)+Ra.\Pr\left(\theta+N\phi\right)-Ha^2.\Pr V \tag{10}$$

$$\frac{\partial \theta}{\partial t'}+U\frac{\partial \theta}{\partial X}+V\frac{\partial \theta}{\partial Y}=\left(\frac{\partial^2 \theta}{\partial X^2}+\frac{\partial^2 \theta}{\partial Y^2}\right)+\gamma\theta \tag{11}$$

$$\frac{\partial \phi}{\partial t'}+U\frac{\partial \phi}{\partial X}+V\frac{\partial \phi}{\partial Y}=\frac{1}{Le}\left(\frac{\partial^2 \phi}{\partial X^2}+\frac{\partial^2 \phi}{\partial Y^2}\right) \tag{12}$$

Using the boundary conditions

Global Digital Central
ISSN: 2151-8629

$$Y = 0: \quad U = V = 0, \quad \frac{\partial \theta}{\partial Y} = 0, \quad \frac{\partial \phi}{\partial Y} = 0 \tag{13}$$

$$Y = 1: \quad U = V = 0, \quad \frac{\partial \theta}{\partial Y} = 0, \quad \frac{\partial \phi}{\partial Y} = 0 \tag{14}$$

$$X = 0: \; U = V = 0, \quad \frac{\partial \theta}{\partial X} = -1, \; \frac{\partial \phi}{\partial X} = -1 \tag{15}$$

$$X = 1: \; U = V = 0, \quad \frac{\partial \theta}{\partial X} = 0, \quad \frac{\partial \phi}{\partial X} = 0 \tag{16}$$

Here $Ha = B_0 L\sqrt{\sigma/\mu}$ is the Hartmann Number, $Le = \alpha / D$ is the Lewis Number, $\Pr = \upsilon/\alpha$ is the Prandtl number, $Ra_T = g\beta\Delta T L^3 \Pr/\upsilon^2$ is the Rayleigh Number, $N = \beta_c \Delta C / \beta_T \Delta T$ is the buoyancy ratio and $\gamma = \varphi_0 L^2/\alpha\rho c_p$ is the dimensionless heat generation or absorption coefficient. The evaluation of stream function (ψ) is using the relationship between velocity components and stream function (ψ) (Batchelor., 1993), the stream function usually defined as $U = \frac{\partial \psi}{\partial Y}$ or $V = -\frac{\partial \psi}{\partial X}$, It may represent that, the positive sign of ψ denotes anti-clockwise circulation and negative sign of ψ denotes clockwise circulation. In all boundaries there is no slip-condition, hence $\psi = 0$ for all boundaries. The heat and mass transfer coefficients in terms of local Nusselt and Sherwood numbers are defined by

$$Nu = -\frac{\partial \theta}{\partial n}, Sh = -\frac{\partial \phi}{\partial n} \tag{17}$$

Where n indicates normal direction of the plane. In addition, the average Nusselt number and Sherwood numbers of the bottom wall are defined as

$$\overline{Nu_b} = \int_0^1 Nu\, dx, \quad \overline{Sh_b} = \int_0^1 Sh\, dx \tag{18}$$

3. NUMERICAL SOLUTION

The dimensionless governing equations (2)-(4) have been solved by the MAC Method (Harlow et al., 1965). In the MAC approach although we consider viscous flow, viscosity is not actually required for numerical stability (Harlow et al., 1965). Cell boundaries are indicated with half-integer values in the finite difference discretization. Here we elaborate on the numerical discretization procedure. Based on the weak conservative form of the unsteady non-linear partial differential equations, we implement a grid meshing procedure using the following notation at the Centre of a cell:

$$u_{i-1/2,j} = \frac{1}{2}\left[u_{i-1,j} + u_{i,j}\right] \tag{19}$$

In X- Momentum conservation i.e., in eqn. (9) we have:

$$\frac{\partial (uu)}{\partial x} = \frac{uu1 - uu2}{\Delta x}$$

Here

$$uu1 = \left[\frac{1}{2}\left(u_{i,j} + u_{i+1,j}\right)\right]^2$$

$$uu2 = \left[\frac{1}{2}\left(u_{i-1,j} + u_{i,j}\right)\right]^2$$

Similarly, we have:

$$\frac{\partial (uv)}{\partial y} = \frac{uv1 - uv2}{\Delta y}$$

where

$$uv1 = \frac{1}{2}\left(u_{i,j} + u_{i,j+1}\right).\frac{1}{2}\left(v_{i,j} + v_{i+1,j}\right)$$

$$uv2 = \frac{1}{2}\left(u_{i,j} + u_{i,j-1}\right).\frac{1}{2}\left(v_{i,j-1} + v_{i+1,j-1}\right)$$

The following central difference formula is used for the second order derivatives:

$$\nabla^2 u = \frac{\partial^2 u}{\partial x^2} + \frac{\partial^2 u}{\partial y^2}$$

$$\nabla^2 u = \frac{u_{i-1,j} - 2u_{i,j} + u_{i+1,j}}{\Delta x^2} + \frac{u_{i,j-1} - 2u_{i,j} + u_{i,j+1}}{\Delta y^2}$$

Applying to the Y-direction momentum conservation eqn. (10) we have:

$$\frac{\partial (vu)}{\partial x} = \frac{vu1 - vu2}{\Delta x}$$

The following notation applies:

$$uv1 = \frac{1}{2}\left(u_{i,j+1} + u_{i,j}\right).\frac{1}{2}\left(v_{i,j} + v_{i+1,j}\right)$$

$$uv2 = \frac{1}{2}\left(u_{i-1,j+1} + u_{i-1,j}\right).\frac{1}{2}\left(v_{i,j} + v_{i-1,j}\right)$$

$$\frac{\partial (vv)}{\partial y} = \frac{vv1 - vv2}{\Delta y}$$

$$vv1 = \left[\frac{1}{2}\left(v_{i,j+1} + v_{i,j}\right)\right]^2$$

$$vv2 = \left[\frac{1}{2}\left(v_{i,j-1} + v_{i,j}\right)\right]^2$$

The central difference formula for the Laplacian operator is given by:

$$\nabla^2 v = \frac{\partial^2 v}{\partial x^2} + \frac{\partial^2 v}{\partial y^2}$$

$$\nabla^2 v = \frac{v_{i-1,j} - 2v_{i,j} + v_{i+1,j}}{\Delta x^2} + \frac{v_{i,j-1} - 2v_{i,j} + v_{i,j+1}}{\Delta y^2}$$

Effectively the X-momentum equation discretization technique can be summarized as:

$$utp = u^n + dt(-A + \Pr.D2\_u)$$

where A = advection term, D2_u = diffusion term = Laplacian of u. There is a slight modification needed in the y-momentum equation due to the addition of a new term. Therefore, this term must be included in the discretized equation and we have:

$$vtp = v^n + dt.(-B + \Pr.D2\_v + Ra.\Pr(\theta + N\varphi) + Ha^2.\Pr V)$$

where B = advection term, D2_v = diffusion term = Laplacian of v. It is further noteworthy that the temperature term T is co-located such that it coincides with velocity before using it in the above equation to account for the staggered grid. After utp and vtp are projected to get u and v, we can use the discretized temperature and concentration equation to get T and ϕ at next time level (T^{n+1}, ϕ^{n+1}) via the algorithm

$$T^{n+1} = T^n + dt(-A\_T + D2\_T + \gamma\theta)$$

$$\phi^{n+1} = \phi^n + dt(-A\_\phi + \frac{1}{Le}.D2\_\phi)$$

where $A\_T, A\_\phi =$ advection term, D2T=diffusion term=Laplacian of T. Next, we integrate in time by an incremental step dt in each iteration until the final time 1.0 is reached. The variables are co-located and plotted. Modern variants of the MAC method utilize the conjugate gradient schemes which solve the Poisson equation. To confirm mesh

Global Digital Central
ISSN: 2151-8629

independence a grid-independence study is conducted. In computational fluid dynamics, of which finite difference simulation is merely one methodology, once a mesh provides a solution which is invariant with the finer meshes, the coarser mesh can be adopted. This reduces computational cost but retains the necessary accuracy. Table 1 shows that accuracy to three decimal places is achieved for Nusselt number at the bottom wall with a mesh of 61 x 61 which is sufficient for heat transfer computations and therefore this is adopted for all subsequent simulations.

Furthermore to corroborate the present computations, visualizations of the temperature (isotherms) and stream function distributions provided. These replicate the solutions of Kandaswamy et al. (2008). the results are in very close correlation, as observed in Fig. 1 (b) and confidence in the present MAC computational code is therefore justifiably high.

4. RESULTS AND DISCUSSIONS

The influence of various values of Rayleigh number (Ra) on the velocity components in the mid-section of square cavity are depicted in Figure.3. It is observed in Fig. 2 that the velocity component increases with enhancement of the Rayleigh number. This is caused by the increased dynamic viscosity, which opposes fluid flow in the cavity. Fig 3. Shows the effect of the Rayleigh number on the streamlines, isotherms and iso-concentration contours for a square enclosure. As seen, flow circular cell is formed at middle of the enclosure for $Ra=10^3$, as the Rayleigh number increases the primary cell moves towards the bottom portion of left vertical wall the shape of the circulation changed to triangular shape. The isotherm lines occupy most of the area inside the cavity, the temperature value smoothly increases to right wall, the effect of Rayleigh number $Ra=10^4$ isotherms are spread over the total cavity, this is caused by increase in buoyancy force. The concentration of the temperature lines is decreased for increased Rayleigh number, the similar effects reflected in iso-concentration contours of the enclosure.

Fig.4a-b depicts the effect of Hartmann number for $Ra=10^4$, Pr=0.7, Le=1.0, N=1.0, and γ=1.0 on the streamlines, isotherms and iso-concentration respectively. The strength of the central stream lines gradually spread throughout the square cavity with increasing the Hartmann number and the streamlines split into two cells, one is formed at the upper (Top) wall and another is formed at the bottom horizontal wall. The nature of flow in the cavity is circular caused by the absence of Hartmann number. The clustered contour maps of isotherms near left vertical wall in the square enclosure for Ha=0, and the isotherm contours are parallel to the vertical walls for Ha=80 and Ha=100. The weak temperature gradients appeared in enclosure for Ha=30 and Ha=50. The iso-concentration gradients are linearly proportional with Hartmann Number, if the Hartmann number is enchased the iso-concentration gradients are reached to constant position in the square cavity that means all the iso-concentration lines are parallel to left and right walls. In the cavity the centerline velocity is fall down with respect to the increased Hartmann number. It is shown in the Figure.5.

Heat generation or absorption (γ) parameter influence on stream lines isotherms and iso-concentration contours with Ha=10, Le=1.0, N=1.0, Pr=0.7 and $Ra=10^4$ shows in Figure.6. Heat and mass transfer is observed for Heat generation or absorption parameter $\gamma = 0, 0.5 \text{ and } 1$. Visual observation of streamlines are noticed there is no significant difference for various values of heat generation or absorption parameter, from the isotherms and iso-concentration contours, its noticed iso-concentration patterns are same for different heat generation or absorption (γ) parameter. Temperature lines are increased when increasing the heat generation or absorption (γ) parameter.

The effect of buoyancy ratio parameter on stream lines, isotherms and iso-concentration contours for uniformly heated left vertical wall with Ha=10, Le=1.0, γ =1.0, Pr=0.7 and $Ra=10^4$ are shows in Figure.7. Heat and mass transfer is observed for buoyancy ratio parameter for N=5, 10 and 15. A single stretched recirculation vortex is formed in the enclosure for N=5, 10 and 15. The buoyancy ratio parameter has been applied it is observed that the primary circulation vortex stretches along the bottom portion of left wall of the cavity. The isotherms are distributed parallel towards horizontal walls. Slight changes are observed in Isotherm patterns for increasing the buoyancy ration parameter (N). Iso-concentration contours patterns are parallel to bottom walls, the patterns are increased for increasing of buoyancy ration parameter (N).

The left wall is maintained at uniform constant heat flux and the remaining all three walls are thermally insulated. In Fi.8a-b, we have depicted the numerical results presented in the form of streamlines, isotherms and iso–concentration contours for various values of Lewis number and for fixed γ=1.0, $Ra=10^4$, N=1.0, Pr=0.7 and Ha=10. The streamline contours are almost nearly same there is no significant change in streamline contours for increasing of Lewis number (Le). It is noticed that dominants regimes of convection Lewis number effect is low. The isotherm contours are not symmetric for different Lewis number, flow pattern lines are gradually increased for increased Le. Iso-concentration lines are changing for various Lewis numbers, the visual observation of iso-concentration contours are forming a vortex for high Lewis number (Le=15). It is noticed that the boundary layer is formed at a left vertical wall for Le=15.

Temperature changes in mid-section of the square enclosure in presence of magnetic effect is exhibited in Figure.9. The temperature of the cavity is varying with Hartmann number, in the absence of magnetic field the value of temperature is low comparing with varying Hartmann number. The flow temperature is linearly increased with increasing of Hartmann number at fixed Prandtl number, The effect of Hartmann number on average Nusselt number and average Sherwood number for varying Heat generation or absorption parameter are seen in Figure.10 when Buoyancy ratio, N=1.0, Le=1.0, $Ra=10^4$ and fixed Pr=0.71. The isotherm gradients are slightly changed for Heat generation parameter at γ=1.0, there is no significant difference of Sherwood number on mass transfer is predicted for γ=0 and 1.0. The present numerical study is wrapped by the Heat and Mass transfer with the effect of Heat generation or absorption parameter (γ) on average Nusselt and Sherwood number for various Rayleigh numbers (Ra) are presented in Figure 11. It is found that the average Nusselt and Sherwood numbers are decreases with increasing of thermal Rayleigh number (Ra) with N=1.0, Le=1.0, Ha=10 and Pr=0.71, the rate of heat transfer increases gradually with increasing of heat generation /absorption coefficient.

Table. 1 Grid independent study

Grid size	Average Nusselt number (Nu)
51 X 51	0.17437
61 X 61	0.17798
71 X 71	0.17319
81 X 81	0.17562

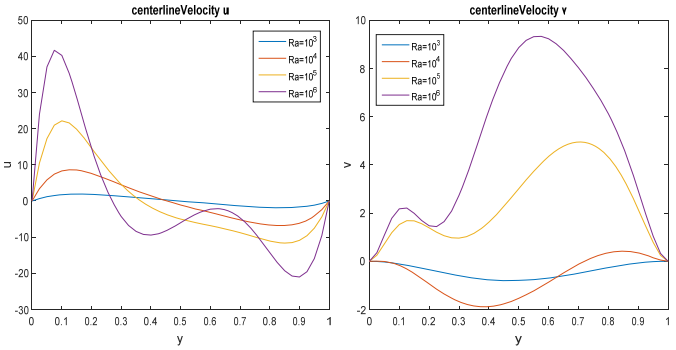

Fig. 2 Effect of Rayleigh number (Ra) on the velocity component at square cavity mid-section with γ=1.0, *Le=1.0, N=1.0, Pr=0.7 and Ha=10*

$Ra=10^3$ $Ra=10^4$

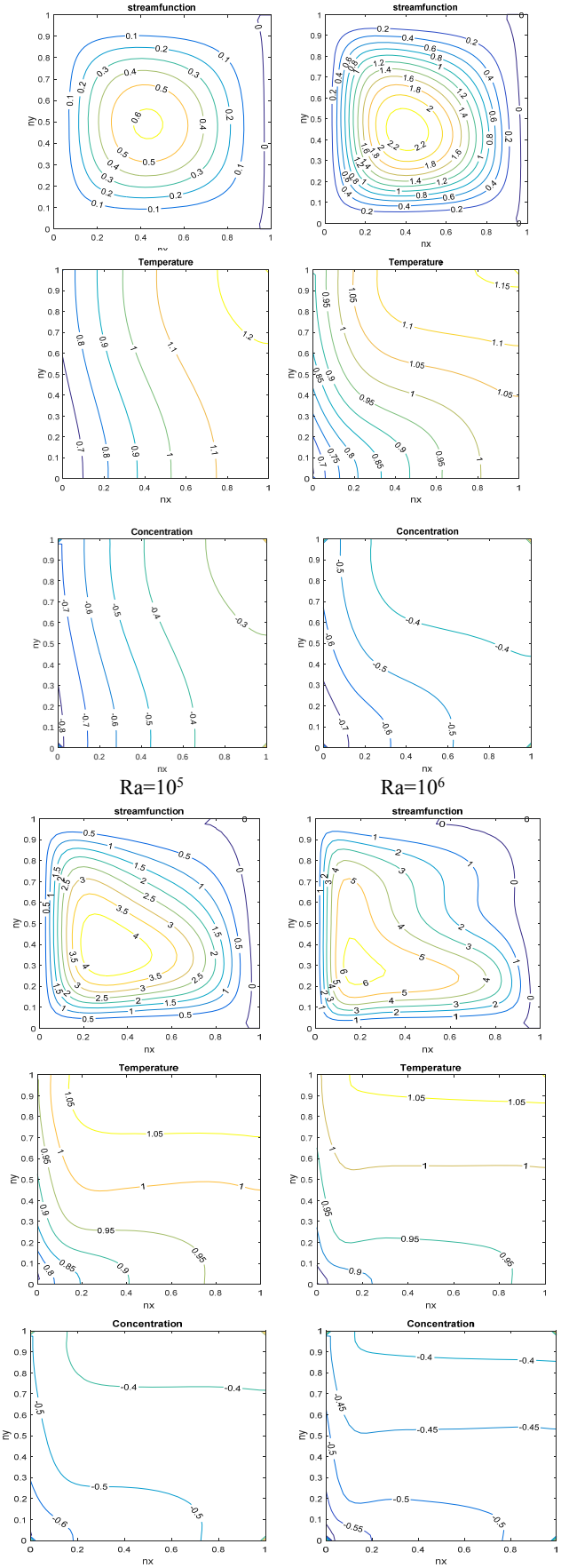

Fig. 2 Effect of Rayleigh number (Ra) on stream lines, isotherms and isoconcentration for γ=1.0, Le=1.0, N=1.0, Pr=0.7 and Ha=10.

Ha=0 Ha=30

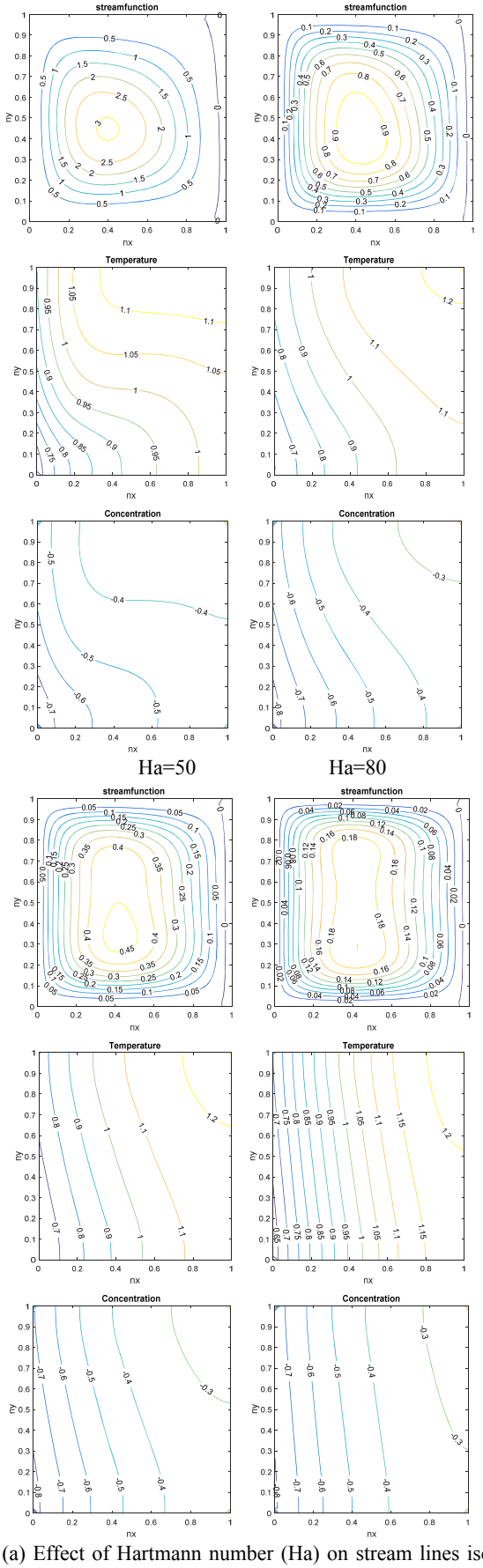

Fig. 4 (a) Effect of Hartmann number (Ha) on stream lines isotherms and iso-concentration contours for γ=1.0, Le=1.0, N=1.0, Pr=0.7 and Ra=10^4 (continue)

Global Digital Central
ISSN: 2151-8629

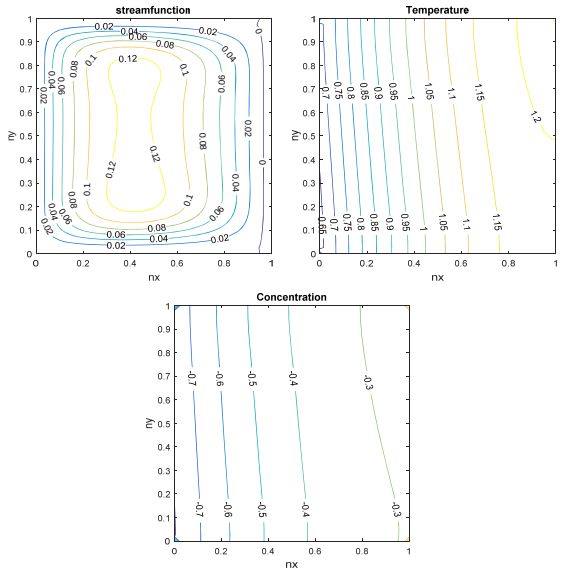

Fig. 4 (b) Stream lines isotherms and iso-concentration contours for Ha=100 with γ=1.0, Le=1.0, N=1.0, Pr=0.7 and Ra=10^4 (continue)

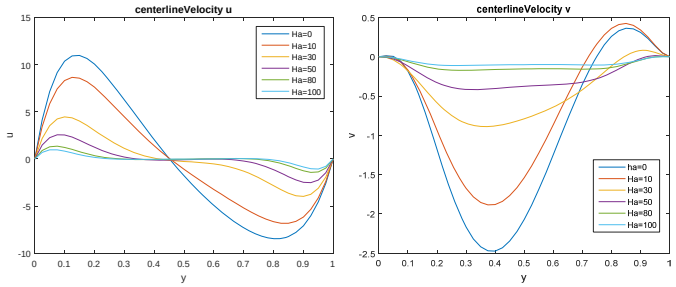

Fig. 5 Effect of Hartmann number on the velocity component at square cavity mid-section with γ=1.0, Le=1.0, N=1.0, Pr=0.7 and Ra=10^4.

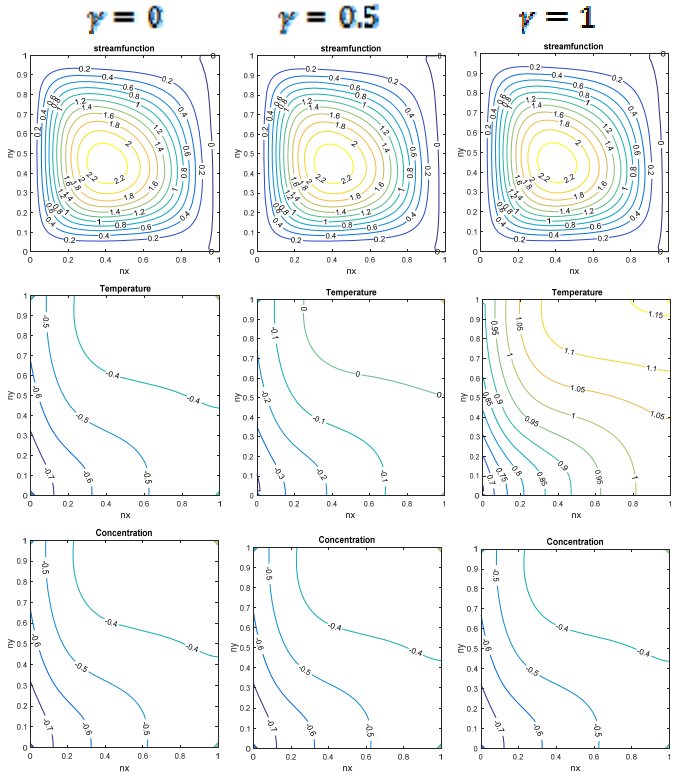

Fig. 6 Effect of Heat generation or absorption (γ) on stream lines isotherms and iso-concentration contours, Ha=10, Le=1.0, N=1.0, Pr=0.7 and Ra=10^4

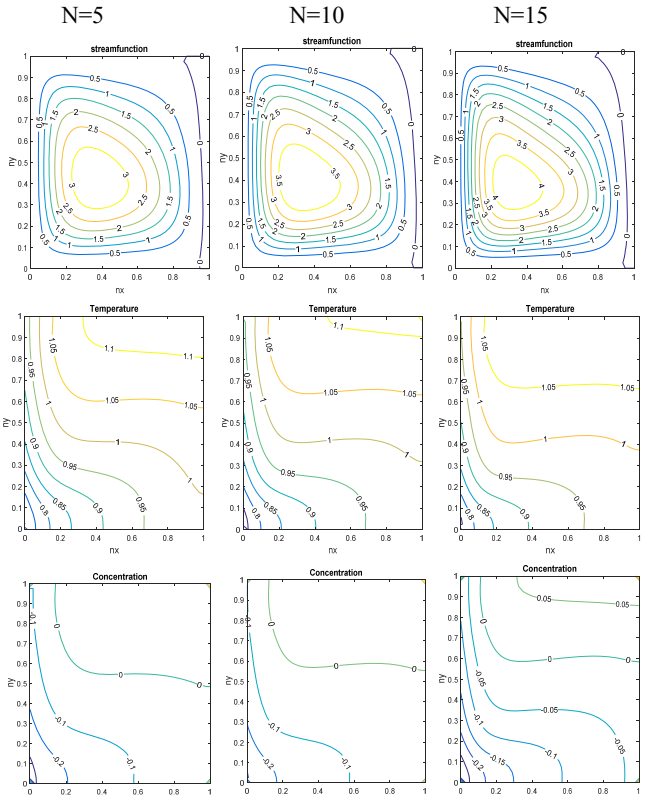

Fig. 7 Effect of buoyancy ratio parameter on stream lines isotherms and iso-concentrations, Ha=10, Le=1.0, γ =1.0, Pr=0.7 and Ra=10^4.

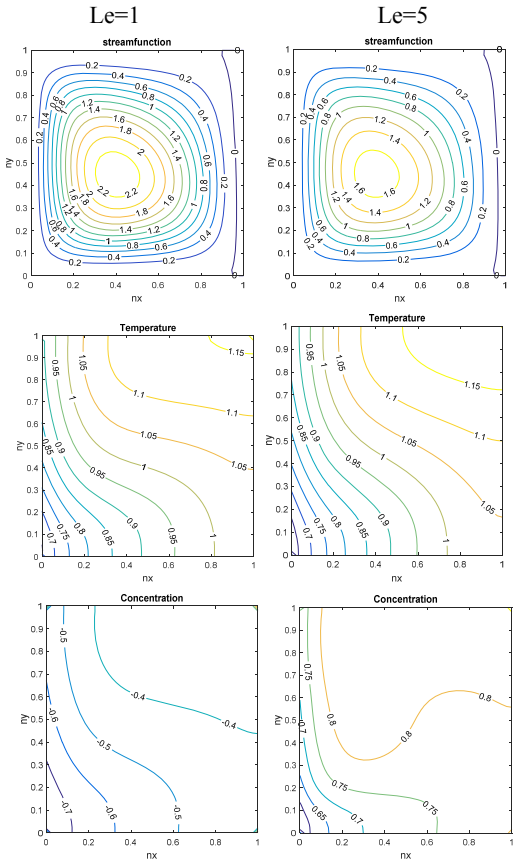

Fig. 8 (a) Effect of Lewis number (Le) on stream lines isotherms and iso-concentration contours, γ=1.0, Ra=10^4, N=1.0, Pr=0.7 and Ha=10, (continue)

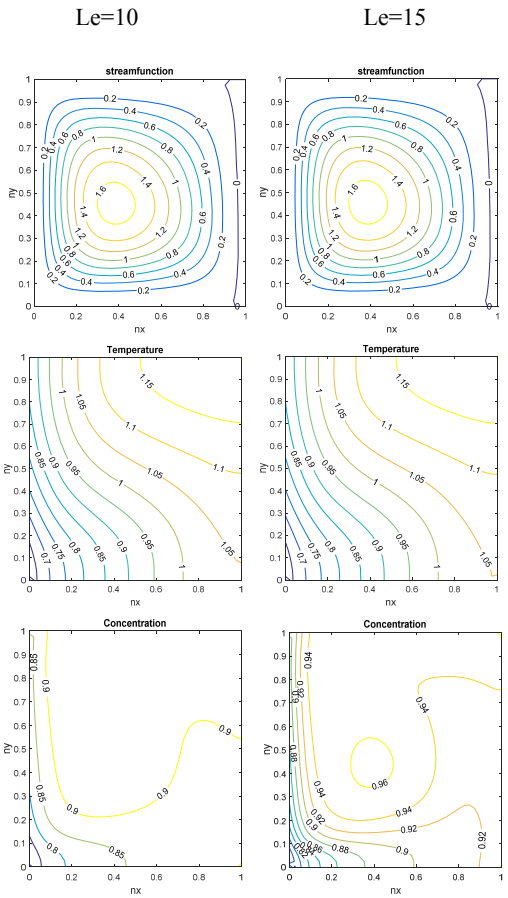

Fig. 8 (b) Effect of Lewis number (Le) on stream lines isotherms and iso-concentration contours, γ=1.0, Ra=10^4, N=1.0, Pr=0.7 and Ha=10.

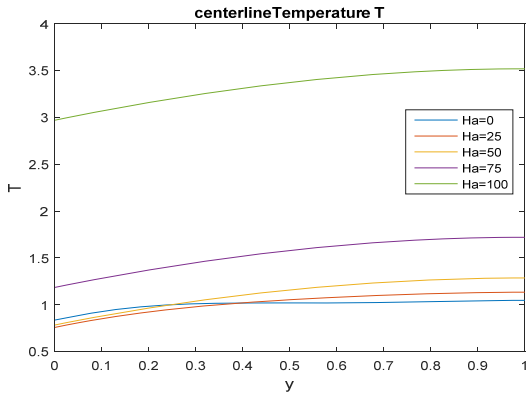

Fig. 9 Effect of Hartmann number (Ha) on mid-section Temperature of square enclosure with γ=1.0, Le=1.0, N=1.0, Pr=0.7, Ra=10^4.

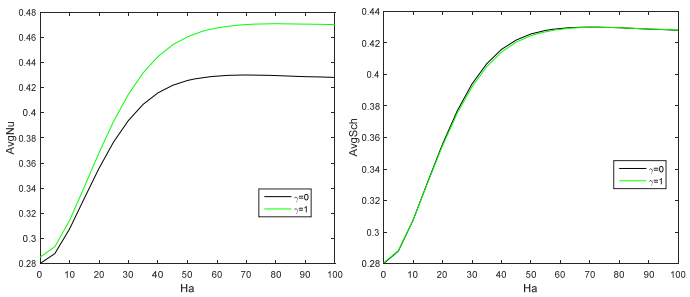

Fig. 10 Effect of Hartmann number (Ha) on average Nusselt and Sherwood number for Le=1.0, N=1.0, Pr=0.7, Ra=10^4.

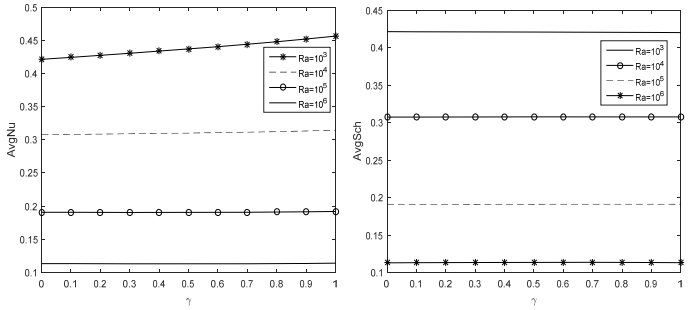

Fig. 11 Effect of Heat generation or absorption (γ) on average Nusselt and Sherwood number Le=1.0, N=1.0, Pr=0.7, Ha=10.

5. CONCLUSIONS

The problem of Double-diffusive convective flow in a square cavity with the effect of magnetic and heat generation or absorption has been studied numerically using MAC Method. The visualized contour results for streamlines, isotherms, iso-concentrations and mid-section velocity fields for various parametric conditions is depicted and discussed. It is observed that the flow characteristics, heat and mass transfer inside the square cavity strongly connected with magnetic field, buoyancy ratio, heat generation/absorption and Lewis number effects. The behavior of mid-section velocity along x-axis is found to be oscillatory nature with increasing the Rayleigh number whereas the behavior of mid-section velocity along y-axis increases. The increase of Hartmann number on mid-section velocity fields along x-axis and y-axis has been found to be the sinusoidal nature and decreasing nature. Increase in Hartmann number leads to increase in average Nusselt and Sherwood numbers and the fluid circulations within the enclosure are found to be decrease. Further, it is noticed that the average Nusselt and Sherwood number increases with the increase of heat generation or absorption. The average Nusselt number gradually increases with increasing the Hartmann number under the influence of Heat generation or absorption parameter. Also, we found that there is no significant change in Sherwood number. It is predicted that the heat and mass transfer rate diminishes by increasing the Rayleigh number and heat generation or absorption parameter.

ACKNOWLEDGEMENTS

The authors appreciate the constructive comments of the reviewers, which led to definite improvement in the paper. The authors are thankful to the management of Madanapalle Institute of Technology & Science, Madanapalle for providing research facilities in the campus.

NOMENCLATURE

B_0	magnetic induction, Tesla
C	dimensionless concentration
c	concentration of species(kg/m3*)*
Cp	specific heat (kJ/kg K)
D	species diffusivity (m2/s)
g	gravitational acceleration(m/s2)
Ha	Hartmann number
k	thermal conductivity (w/mk)
L	width of enclosure, m
Le	Lewis number
N	buoyancy ratio
Nu	Nusselt number
p	fluid pressure(pa)
P	dimensionless fluid pressure
Pr	Prandtl number
q'	heat flux(W/m2)
q^*	mass flux(W/m2*)*
Ra	Rayleigh number
Sh	*local Sherwood number*

t	time(s)
t'	*dimensionless time (s)*
T	temperature(k)
u	horizontal velocity(m/s)
U	dimensionless horizontal velocity
v	vertical velocity(m/s)
V	dimensionless vertical velocity
x,y	dimensional coordinates (m)
X,Y	dimensionless coordinates

Greek Symbols

υ	kinematic viscosity, m^2/s
μ	dynamic viscosity, kg/m s
σ	electric conductivity
α	thermal diffusivity, m^2/s
ρ	fluid density, kg/m^3
ϕ	dimensionless mass concentration
θ	dimensionless temperature
ψ	streamfunction
β_T	coefficient of thermal expansion, k^{-1}
β_c	coefficient of solutal expansion, m^3/kg
φ_0	heat generation or absorption coefficient
γ	dimensionless heat generation or absorption coefficient

REFERENCES

Ali Mchirgui, Nejib Hidouri, Mourad Magherbi, Ammar Ben Brahim, 2014, "Finite Element Analysis of Second Law in Double Diffusive Natural Convection Through an Inclined Porous Cavity," *Computers & Fluids*, 96, 105–115.

https://doi.org/10.1016/j.compfluid.2014.03.008

Batchelor, G.K., 1993, "An Introduction to Fluid Dynamics," Cambridge University Press, Cambridge.

Chandra Shekar Balla, Kishan Naikoti, 2015, "Soret and Dufour Effects On Free Convective Heat and Solute Transfer in Fluid Saturated Inclined Porous Cavity," *Eng. Sci. Tech., an Int. J.*, **18**(4), 543-554.
https://doi.org/10.1016/j.jestch.2015.04.001

Davis, D.V., 1983, "Natural Convection of Air in a Square Enclosure: A Benchmark Numerical Solution," *Int. J. Num. Meth. Fluids*, **3**(3), 249–264.
https://doi.org/10.1002/fld.1650030305

Elshehabey, H.M., Ahmed, S.E., 2015, "MHD Mixed Convection in A Lid-Driven Cavity Filled by A Nanofluid with Sinusoidal Temperature Distribution on The Both Vertical Walls Using Buongiorno's Nanofluid Model," *Int. J. of Heat and Mass Transfer*, **88**, 181–202.
https://doi.org/10.1016/j.ijheatmasstransfer.2015.04.039

Ghasemi, B., Aminossadati, S. M., Raisi, A., 2011, "Magnetic Field Effect on Natural Convection in A Nanofluid-Filled Square Enclosure," *Int. J. Ther. Sci.*, **50**(9), 1748-1756.
https://doi.org/10.1016/j.ijthermalsci.2011.04.010

Han, H., Kuehn, T.H., 1991, "Double-Diffusive Natural Convection in A Vertical Rectangular Cavity: I. Experimental Study," *Int. J. Heat and Mass Transfer*, **34**, 449–459.
https://doi.org/10.1016/0017-9310(91)90264-F

Hillal M. Elshehabey, Sameh E. Ahmed, 2015, "MHD Mixed Convection in A Lid-Driven Cavity Filled by a Nanofluid with Sinusoidal Temperature Distribution on the Both Vertical Walls Using Buongiorno's Nanofluid Model," *Int. J. Heat and Mass Transfer*, **88**, 181–202.
https://doi.org/10.1016/j.ijheatmasstransfer.2015.04.039

Harlow F.H., and Welch, J.E., 1965, "Numerical Calculation of Time-Dependent Viscous Incompressible Flow of Fluid with Free Surface," *Physics of Fluids*, **8**(12), 2182-2190.
http://dx.doi.org/10.1063/1.1761178

Kakarantzas, S. C., Sarris, I. E. and Vlachos, N. S., 2014, "Magnetohydrodynamic Natural Convection of Liquid Metal between Coaxial Isothermal Cylinders due to Internal Heating," *Numerical Heat Transfer, Part A*, **65**(5), 401–418.
http://dx.doi.org/10.1080/10407782.2013.831681

Kandaswamy, P., Muthtamilselvan, M., Lee, J., 2008, "Prandtl Number Effects on Mixed Convection in A Lid-Driven Porous Enclosure," *Journal Porous Media*, **11**(8), 791–801.

Kefayati, GH.R., 2014, "Mesoscopic Simulation of Magnetic Field Effect on Double-Diffusive Mixed Convection of Shear-Thinning Fluids in A Double Lid Driven Cavity," *J. Mol. Liq.*, **198**, 413–429.
https://doi.org/10.1016/j.molliq.2014.07.024

Litan Kumar Saha, Monotos Chandra Somadder, Nepal Chandra Roy, 2015 "Hydro-magnetic Mixed Convection Flow in A Lid-Driven Cavity with Wavy Bottom Surface," *American J. App. Math.*, **3**(1), 8-19.
doi:10.11648/j.ajam.s.2015030101.12

Lambert T.A., Murphy K.D., 2002, "Modal Convection and Its Effect on The Stability of EDM Wires," *Int. J. Mech. Sci.*, **44**, 207–216.
https://doi.org/10.1016/S0020-7403(01)00075-3

Murphy, K.D., Lin, Z.M., 2000, "The Analysis of Spatially Non Uniform Temperature Fields Influence on the Vibration and Stability Characteristics of EDM Wires," *Int. J. Mech. Sci.*, **42**, 1369–90.
https://doi.org/10.1016/S0020-7403(99)00064-8

Mchirgui, A., Hidouri, N., Magherbi, M., Brahim, A.B., 2012, "Entropy Generation in Double-Diffusive Convection in A Porous Cavity Using Darcy-Brinkman Formulation," *Transp Porous Med*, **93**(1), 223–240.
https://doi.org/10.1007/s11242-012-9954-7

Mohan, C. G., Satheesh, A., 2016, "The Numerical Simulation of Double-Diffusive Mixed Convection Flow in a Lid-Driven Porous Cavity with Magnetohydrodynamic Effect," *Arabian Journal for Science and Engineering*, **41**(5), 1867–1882
https://doi.org/10.1007/s13369-015-1998-x

Makayssi, T., Lamsaadi, M., Naimi, M., Hasnaoui, M., Raji, A., Bahlaoui, A., 2008, "Natural Double-Diffusive Convection in A Shallow Horizontal Rectangular Enclosure Uniformly Heated and Salted from The Side and Filled with Non-Newtonian Power-Law Fluids: The Cooperating Case," *Energy Conversion and Management*, **49**(8), 2016-2025.
https://doi.org/10.1016/j.enconman.2008.02.008

Mohamed A. Teamah, Ahmed F, Elsafty, Enass Z, Massoud, 2012, "Numerical Simulation of Double-Diffusive Convective Flow in an Rectangular Enclosure under Magnetic Field and Heat Source," *Int. J. Ther. Sci.*, **52**, 161-175.
https://doi.org/10.1016/j.ijthermalsci.2011.09.006

Ostrach, A., 1988, "Natural Convection in Enclosures," *Journal of Heat Transfer*, **110**(4b), 1175–1190.

Global Digital Central
ISSN: 2151-8629

Pei, Y.C., Ouyang, H., Wang CH., 2014, "Dynamic Interaction of Heat Transfer, Air Flow and Disc Vibration of Disc Drives — Theoretical Development and Numerical Analysis," *Int. J. Mech. Sci.*, **89**, 362–380. https://doi.org/10.1016/j.ijmecsci.2014.09.010

Sun, H., Lauriat, G., Sun, D.L., Tao, W.Q., 2010, "Transient Double-Diffusive Convection in an Enclosure with Large Density Variations," *Int. J. Heat and Mass Trans*, **53**(4), 615–625. https://doi.org/10.1016/j.ijheatmasstransfer.2009.10.035

Sheikholeslami, M., Gorji-Bandpy, M., Ganji, D.D., Soheil Soleimani, 2014, "Heat Flux Boundary Condition for Nanofluid Filled Enclosure in Presence of Magnetic Field," *J. Mol. Liq.*, **193**, 174-184. https://doi.org/10.1016/j.molliq.2013.12.023

Sathiyamoorthy, M., Chamkha, Ali J., 2012, "Natural Convection Flow under Magnetic Field in a Square Cavity for Uniformly (Or) Linearly Heated Adjacent Walls," *Int. J. Num. Meth. Heat & Fluid Flows*, **22**(5), 677-698. https://doi.org/10.1108/09615531211231307

Sivasankaran, S., Malleswaran, A., Lee, J. and Sundar, P., 2011, "Hydro-magnetic Mixed Convection in a Lid-Driven Enclosure with Sinusoidal Boundary Conditions on both Sidewalls," *Int. J. Heat and Mass Trans.*, **54**, 512-525. https://doi.org/10.1016/j.ijheatmasstransfer.2010.09.018

Tapas Ray Mahapatra, Dulal Pal, Sabyasachi Mondal, 2013, "Effects of Buoyancy Ratio on Double-Diffusive Natural Convection in a Lid-Driven Cavity," *Int. J. Heat and Mass Trans.*, **57**(2), 771–785. https://doi.org/10.1016/j.ijheatmasstransfer.2012.10.028 .